Supplemental Information

Cytochrome P450 11A1-Mediated Bioactivation of a Kinase Inhibitor in Rats. Use of Metabolite Radioprofiling, Modulation of Metabolism and Adrenocortical Cell Lines to Evaluate Adrenal Toxicity Potential

Donglu Zhang, Oliver Flint, Lifei Wang, Ashok Gupta, Richard Westhouse, Weiping Zhao, Nirmala Raghavan, Janet Caceres-Cortes, Punit Marathe, Guoxiang Shen, Yueping Zhang, Alban Allentoff, Jonathan Joseph, Jinping Gan, Robert Borzilleri, W Griffith Humphreys

Table of Contents

Metabolite Identification

M4. This metabolite had a molecular ion $[M+H]^+$ at m/z 651 (459+16+176) and showed fragment ions at m/z 475 and 216 (Table 4). M4 was proposed as a glucuronide conjugate of a hydroxylated metabolite (modification on the B substructure).

M5 and M26. Metabolite M5 and M26 were detected by LC/MS/MS in bile and urine samples and showed the same molecular $[M+H]^+$ at m/z 475 (459+16) and fragment ions at m/z 234, 216, 188, and 160 that were the same as those of the parent compound. M26 and M5 were assigned as hydroxylated metabolites (proposed modification on the B substructure).

M6. This metabolite had a molecular ion $[M+H]^+$ at m/z 651 (459+16+176) and showed fragment ions at m/z 475, 408, 250, 232 (216+16), and 204 (Table 4). M6 was assigned as a glucuronide conjugate of a hydroxylated metabolite (proposed modification on the A substructure).

M7. This metabolite had a molecular ion $[M+H]^+$ at m/z 651 (459+16+176) and showed fragment ions at m/z 475 and 232 (Table 4). M7 was a glucuronide conjugate of a hydroxylated metabolite (proposed modification on the A substructure).

M8 and M9. This two metabolite had a molecular ion $[M+H]^+$ at m/z 635 (459+176) and showed fragment ions at m/z 619 or 617 (635-18) and 459 (Table 4). M8 and M9 were glucuronide conjugates of parent compound.

M10. This metabolite had a molecular ion $[M+H]^+$ at m/z 343 and showed fragment ions at m/z 325, 234, and 216 (Table 4). M10 was consistent with an *O*-dearylation of parent compound.

M11. Metabolite M11 had a molecular ion $[M+H]^+$ at m/z 475 and showed fragment ions at m/z 232 (216+16), 204 (188+16), and 176 (160+16). M11 was identified as a hydroxylated metabolite (proposed modification on the A substructure).

M12 and M17. Metabolite M12 and M17 showed the same molecular ions $[M+H]^+$ at m/z 507 (M+3x16) and major fragment ions at m/z 463, 435, 343, 325, 234, and 216. The two metabolites were identified as a trihydroxylated BMS-A (proposed modification on the B substructure).

M13. Metabolite M13 had a molecular ion $[M+H]^+$ at m/z 651 and fragment ions at m/z 633 (651-18), 615, 475 (459+16), 408, 232, and 204. Metabolite M13 was identified as a glucuronide conjugate of a hydroxylated metabolite (proposed modification on the A substructure).

M14. Metabolite M14 had a molecular ion $[M+H]^+$ at m/z 475 and showed fragment ions at m/z 457 (475-18), 232 (216+16), 204 (188+16), and 176 (160+16). Metabolite M14 was identified as a hydroxylated metabolite (proposed modification on the A substructure).

M15. Metabolite M15 had a molecular ion $[M+H]^+$ at m/z 651 and showed fragment ions at m/z 475 (651-176), 408, 250 (234+16), and 232 (216+16). Metabolite M15 was

identified as a glucuronide conjugate of a hydroxylated metabolite (proposed modification on the A substructure).

M16. Metabolite M16 had a molecular ion $[M+H]^+$ at m/z 475 and showed fragment ions at m/z 250 (234+16), 232 (216+16), and 176 (160+16). Metabolite M16 was identified as a hydroxylated metabolite (proposed modification on the A substructure).

M18 and M19. Metabolite M18 and M19 had molecular ions $[M+H]^+$ at m/z 491 and fragment ions at m/z 473 (491-18), 250 (234+16), 232 (216+16), and 176 (160+16). Metabolite M18 and M19 were identified as dihydroxylated metabolites (proposed modifications on the A and B substructures).

M20 and M21. Metabolites M20 and M21 had a molecular ions $[M+H]^+$ at m/z 491 and showed fragment ions at m/z 473 (491-18), 234, 216, and 188. M20 and M21 were identified as dihydroxylated metabolites (both modification proposed on the B substructure).

M22, M23, and M24. M22, M23, and M24 had the same molecular ions $[M+H]^+$ at m/z 667 and fragment ions at m/z 649, 491, 408, and 232. These three metabolites were identified as glucuronide conjugates of dihydroxylated metabolites (proposed modification on the A and B substructures).

M25. Metabolite M25 was detected by LC/MS/MS and showed a molecular ion $[M+H]^+$ at m/z 234 and fragment ions at m/z 216, 188, and 160 (Table 4). M25 had the same HPLC retention time and identical fragments as a synthetic metabolite standard. M25 was assigned as an amide hydrolysis metabolite. This hydrolysis pathway also formed a non-radioactive amino metabolite that was not detected in this study.

Table 1S. Recovery of radioactivity in bile, urine, feces, and GI tract of BDC rats following oral administration of [^{14}C]BMS-A (15 mg/kg, 199.5 μCi/kg)

Group		Recovery of radioactivity (% of dose)					
		Urine	Feces	Bile	GI	Cage Wash	Total
BMS-A-treated	Rat 1	1.42	2.35	33.5	27.5	0.25	65.0
	Rat 2	1.88	9.49	35.0	11.9	0.23	58.5
	Rat 3	2.29	16.0	17.7	11.8	3.65	51.5
	Mean	1.86	9.29	28.7	17.08	1.38	58.3
	SD	0.44	6.84	9.59	9.01	1.97	6.76
BMS-A/ ABT-treated	Rat 4	1.83	8.31	14.2	10.7	0.27	35.3
	Rat 5	2.48	1.00	3.26	9.86	0.43	17.0
	Rat 6	3.89	2.95	7.08	9.11	0.41	23.4
	Mean	2.73	4.09	8.18	9.89	0.37	25.3
	SD	1.05	3.79	5.55	0.80	0.09	9.27

Table 2SA. Relative percent distribution of radioactivity among various peaks in the radiochromatographic profiles of pooled BMS-A-treated rat bile, urine, and feces after oral administration of [^{14}C]BMS-A (15 mg/kg, 199.5 μCi/kg)

Metabolite		Relative distribution (% sample) [a]			Relative distribution (% dose) [b]		
M	$[M+H]^+$	Bile	Urine	Feces	Bile	Urine	Feces
M1	475	2.1	0.3	19	0.6	0.01	1.7
M17	507	2.4	7.0	-	0.7	0.13	-
M25	234	3.2	9.7	1.3	0.9	0.18	0.12
M26	475	4.0	4.3	1.9	1.2	0.08	0.18
M4	651	9.7	5.3	-	2.8	0.1	-
M5	475	19	11	-	5.4	0.19	-
M6	651	4.1	3.4	-	1.2	0.06	-
M7	651	3.1	2.1	-	0.9	0.04	-
M8	635	1.9	ND [c]	-	0.5	ND	-
M9	635	2.0	1.1	-	0.6	0.02	-
M10	343	3.1	2.4	-	0.9	0.05	-
M11	475	3.3	0.7	-	1.0	0.01	-
M12	507	3.2	1.4	-	0.9	0.03	-
M13	651	1.6	ND	-	0.5	ND	-
M14	475	ND	2.2	-	ND	0.04	
M15	651	ND	3.0	-	ND	0.06	-
M16	475	ND	6.0	-	ND	0.10	-
M18	491	Trace [d]	Trace	3.3	-	-	0.30
M19	491	Trace	Trace	-	-	-	-
M20	491	Trace	Trace	-	-	-	-
M21	491	Trace	Trace	-	-	-	-
M22	667	Trace	Trace	-	-	-	-
M23	667	Trace	Trace	-	-	-	-
M24	667	Trace	Trace	-	-	-	-
P (BMS-A)	459	6.7	1.0	53	1.9	0.01	4.9
Total		69	61	78	20	1.1	7.2

[a] Radioactive peaks are reported as a percentage of the total radioactivity eluted from the column after background subtraction. [b]Radioactive peaks are reported as a percentage of the radioactive dose.

[c] ND = not determined. [d]Trace amounts by radioactivity but detectable by MS.

Table 2SB. Relative percent distribution of radioactivity among various peaks in the radiochromatographic profiles of pooled BMS-A/ABT-treated rat bile, urine, and feces after oral administration of [^{14}C]BMS-A (15 mg/kg, 199.5 μCi/kg)

Metabolite		Relative distribution (% sample) [a]			Relative distribution (% dose) [b]		
M	$[M+H]^+$	Bile	Urine	Feces	Bile	Urine	Feces
M1	475	2.2	0.1	12	0.18	Trace	-
M17	507	4.0	3.9	-	0.33	0.11	-
M25	234	2.9	6.8	Trace [c]	0.24	0.19	-
M26	475	7.4	8.4	Trace	0.61	0.23	-
M4	651	20	2.1	-	1.6	0.06	-
M5	475	ND	25	-	ND	0.69	-
M6	651	20	ND [d]	-	1.6	ND	-
M7	651	2.7	2.6	-	0.22	0.07	-
M8	635	1.5	0.9	-	0.13	0.03	-
M9	635	1.7	ND	-	0.14	ND	-
M10	343	2.9	ND	-	0.24	ND	-
M11	475	3.1	1.2	-	0.25	0.03	-
M12	507	1.9	2.2	-	0.16	0.06	-
M13	651	1.5	ND	-	0.12	ND	-
M14	475	ND	2.2	-	ND	0.06	-
M15	651	ND	1.2	-	ND	0.03	-
M16	475	ND	6.2	-	ND	0.17	-
M18	491	Trace	Trace	Trace	-	-	-
M19	491	Trace	Trace	-	-	-	-
M20	491	Trace	Trace	-	-	-	-
M21	491	Trace	Trace	-	-	-	-
M22	667	Trace	Trace	-	-	-	-
M23	667	Trace	Trace	-	-	-	-
M24	667	Trace	Trace	-	-	-	-
P (BMS-A)	459	2.6	1.0	86	0.21	0.04	3.5
Total		74	63	97	6.1	1.8	4.0

[a] Radioactive peaks are reported as a percentage of the total radioactivity eluted from the column after background subtraction.

[b] Radioactive peaks are reported as a percentage of the radioactive dose.

[c] Trace amounts by radioactivity and detectable by LC/MS.

[d] ND = not determined.

Figure 1S. Modified after Rainey et al., Mol Cell End, 228: 23-38 and Stewart in William's Textbook of Endocrinology, Larsen et al., Eds.

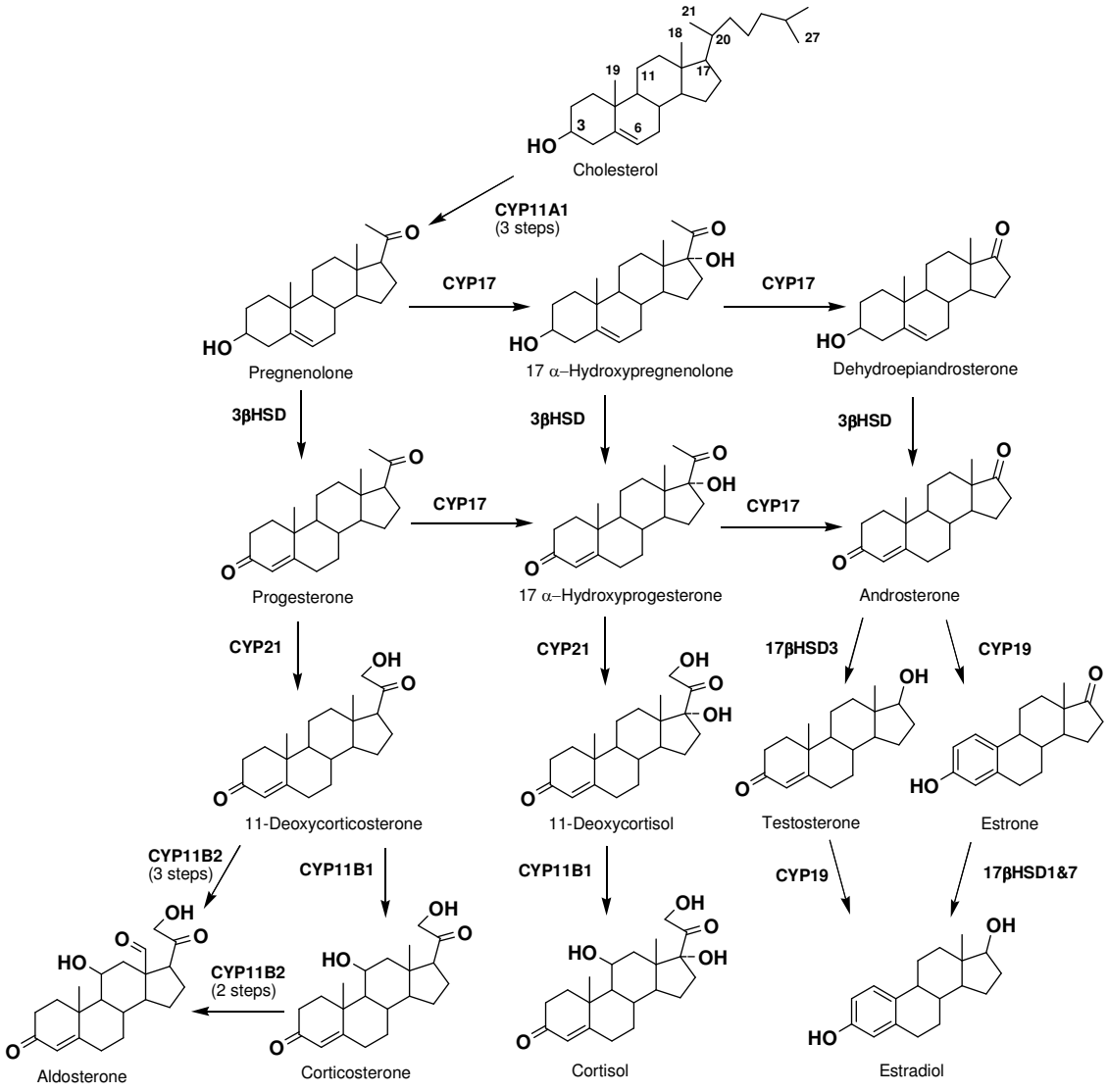

Figure 2SA. Adrenal cortex of a rat following single daily oral doses of 10 mg/kg BMS-A for 7 days

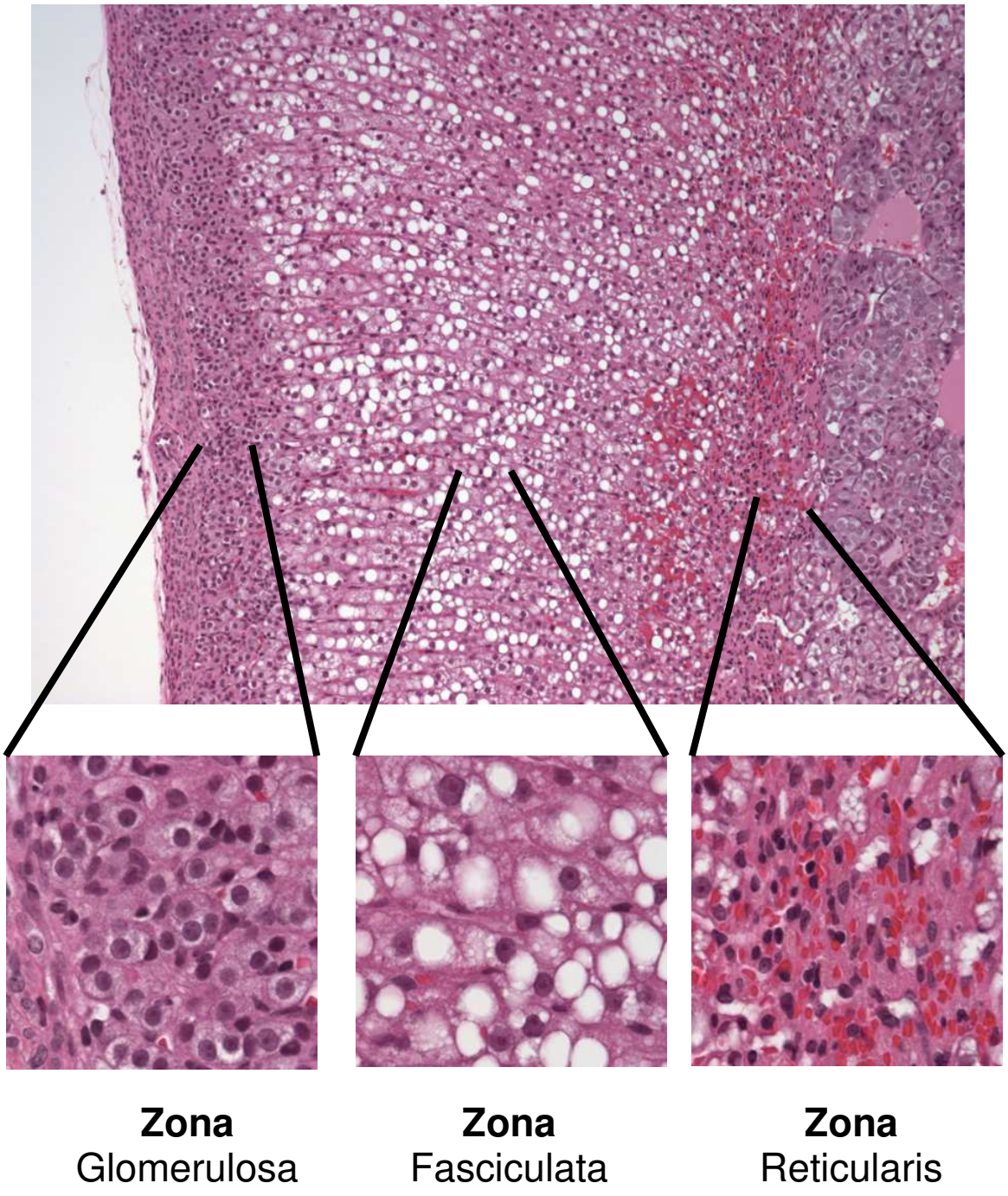

Figure 2SB. Adrenal cortex of a rat following a single oral dose of 30 mg/kg BMS-A

Figure 3SA: Profiles of radioactivity in bile of rats following oral administration of [^{14}C]BMS-A (15 mg/kg, 199.5 μCi/kg) with and without pretreatment of ABT (1,2,3....= M1, M2, M3....)

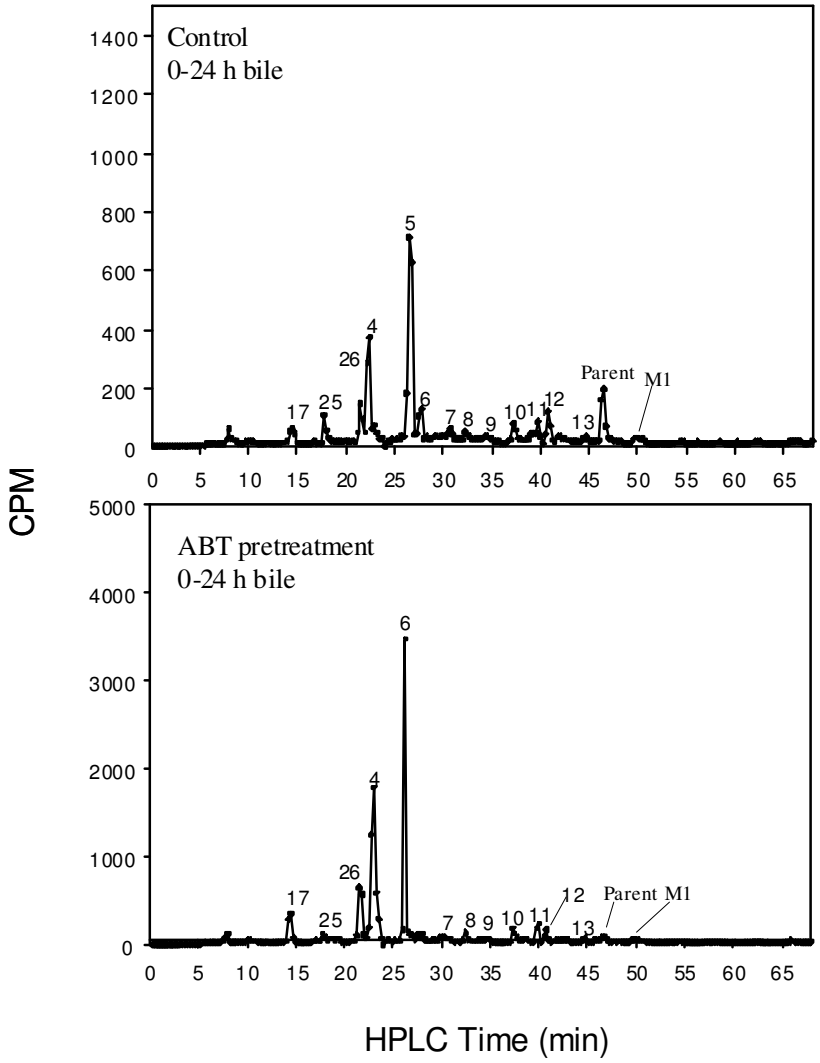

Figure 3SB: Profiles of radioactivity in urine of rats following oral administration of [^{14}C]BMS-A (15 mg/kg, 199.5 μCi/kg) with and without pretreatment of ABT (1,2,3....=M1, M2, M3....)

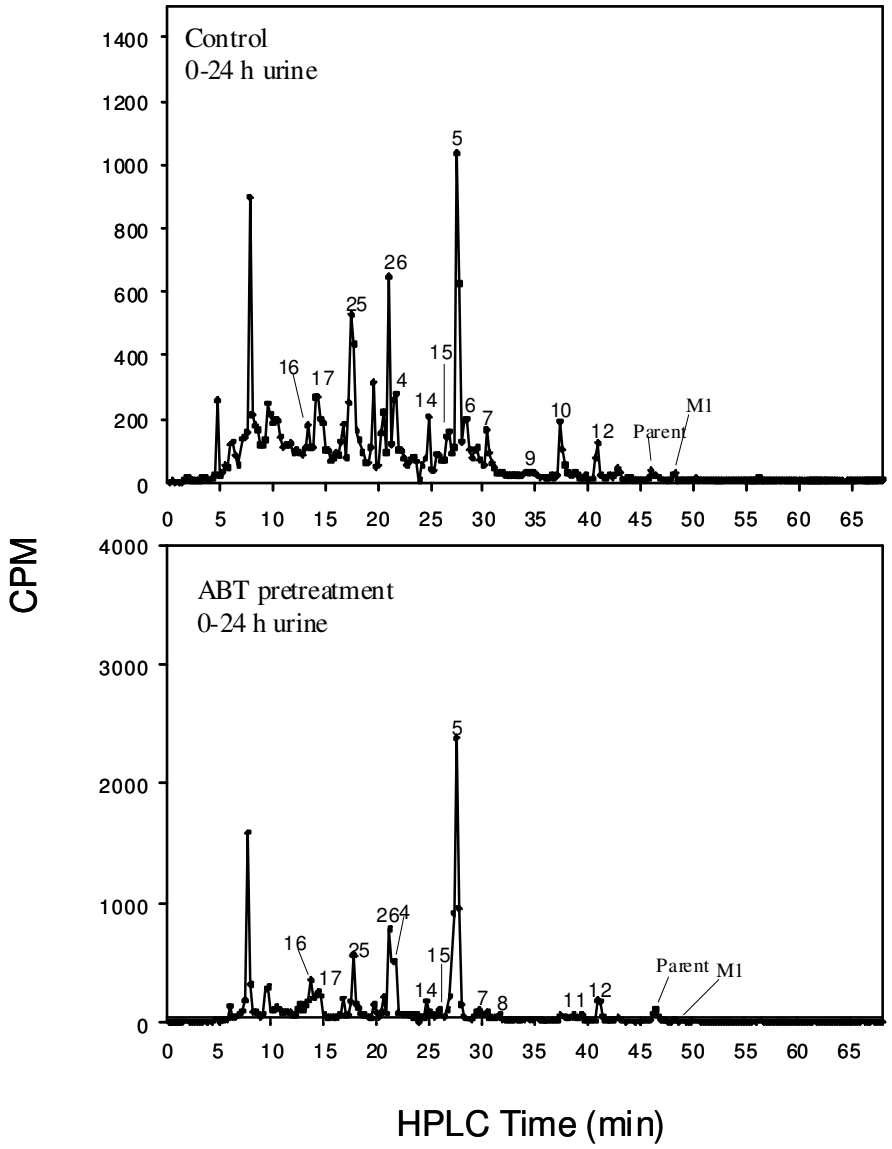

Figure 3SC: Profiles of radioactivity in feces of rats following oral administration of [^{14}C]BMS-A (15 mg/kg, 199.5 μCi/kg) with and without pretreatment of ABT (1,2,3....=M1, M2, M3....)

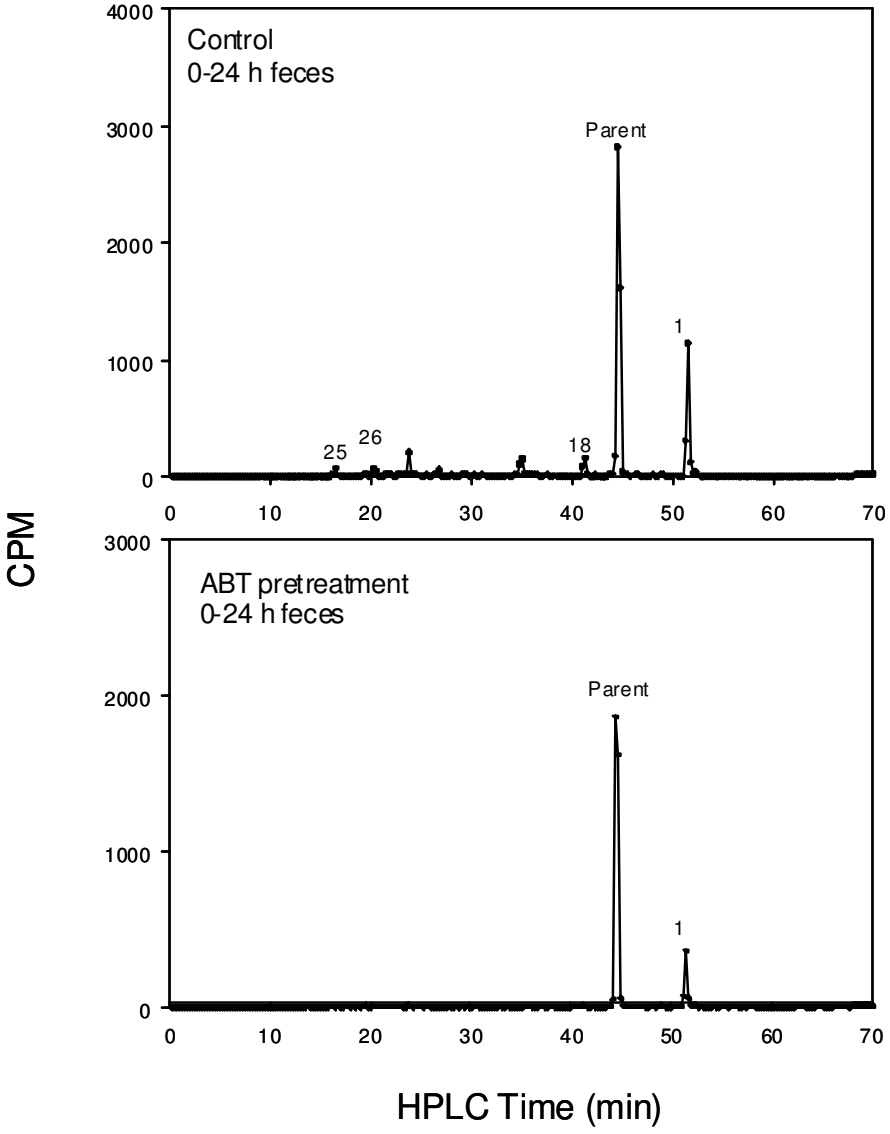

Figure 4SA. HPLC profiles of radioactivity in rat plasma from the untreated group after oral administration of [^{14}C]BMS-A (15 mg/kg, 199.5 μCi/kg)

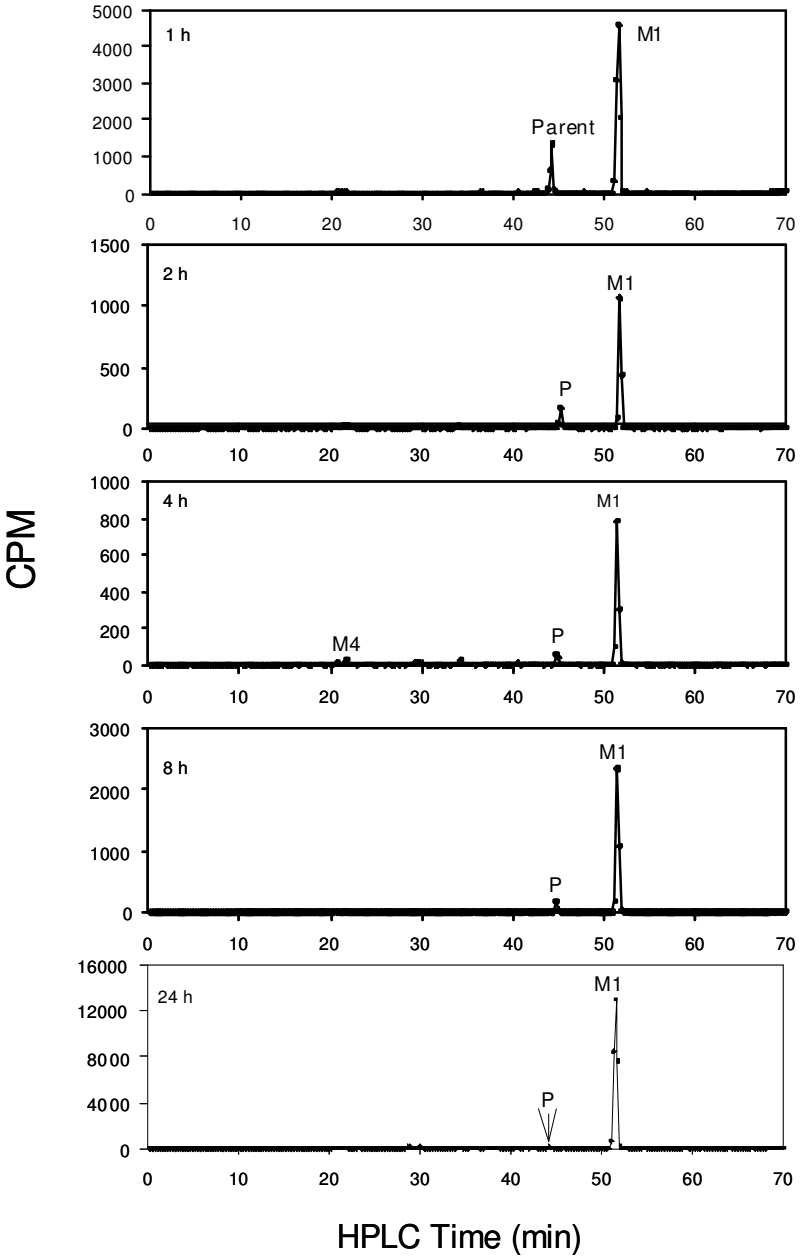

Figure 4SB. HPLC profiles of radioactivity in plasma from ABT-pretreated group after oral administration of [^{14}C]BMS-A (15 mg/kg, 199.5 μCi/kg)

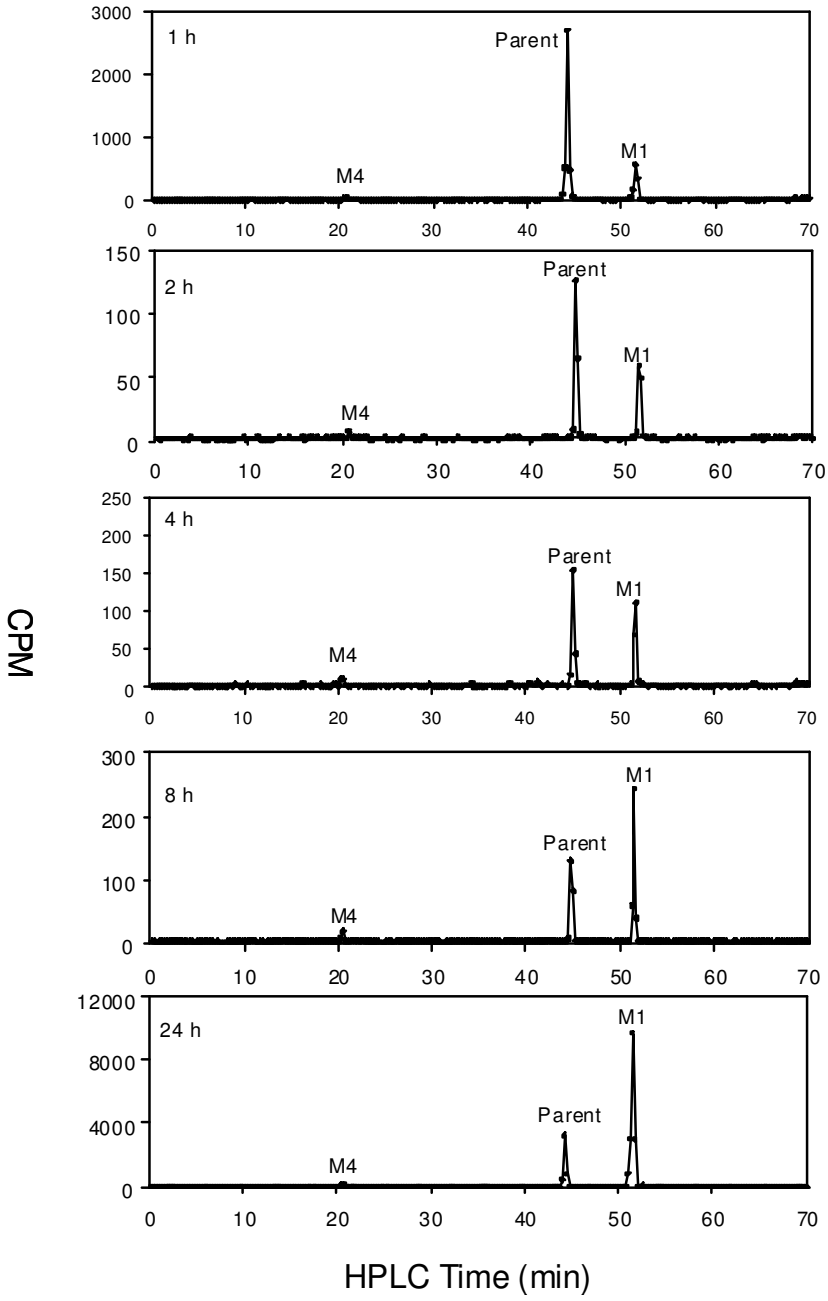

Figure 5S. Metabolite profiles of radioactivity in the medium after a 24h incubation of [^{14}C]BMS-A (10 μM) with Y1 cell cultures